Insight Into the effect of halogen X in Methylammonium Lead Halide ($MAPbX_3$) Spin-Coated on Zinc Oxide film

Klègayéré Emmanuel Koné[1*], Amal Bouich[1,3], Júlia Marí-Guaita[1], Bernabé Marí Soucase[1], and Donafologo Soro[2]

[1]*Departament de Física Applicada, Instituto de diseño y Fabricació (IDF), Universitat Politècnica de València (UPV), Cami vera, Spain.*

[2]*Département des Sciences et Technologie, Ecole Normale supérieure (ENS) d'Abidjan, Cocody, Côte d'ivoire.*

[3]*Física Applicada a las Ingeniereas aeronáutica Naval & Instituto de Energía Solar, Universidat politécnica de Madrid, Spain*

[*]*Email: koneemmanuel277@gmail.com*

Abstract

Herein, we investigated the effect of halogen X in methylammonium lead halide ($MAPbX_3$) where X = (Iodide / Bromide, or Chloride) deposited by spin coating technique on a zinc oxide layer. The ZnO films were first deposited on Fluorine-doped Tin Oxide (FTO) substrates. Then, the perovskite solutions ($MAPbI_3$, $MAPbBr_3$, and $MAPbCl_3$) were deposited on the ZnO layer. The films obtained were characterized by X-ray diffraction (XRD), UV-Visible spectroscopy, and Scanning Electron Microscopy (SEM). The XRD analysis shows characteristic peaks of the ZnO/$MAPbX_3$ heterojunction corresponding to the (100) and (200). The ZnO/$MAPbBr_3$ peaks are more intense than other sample peaks. This analysis also shows the crystalline character of the films produced. SEM images also show the good crystallinity of the films produced. The images show that the grain sizes of the sample ZnO/$MAPbBr_3$ are the largest compared to others. The UV-visible characterization showed that the iodine-based sample absorbed better and had a good band gap (Eg = 1.95 eV). The degradation study was carried out after two weeks of the deposition. The results showed that the iodine-based sample degrades faster compared to another halogen. These findings are helpful in producing stable and efficient perovskite-based solar cells.

Keywords: Spin coating**,** ZnO/$MAPbX_3$, Optical properties, XRD, Degradation

1- Introduction

Recently, Photovoltaic energy has known lot of intention, the discovery of a new material that is a potential candidate for the development of solar cells. Indeed, the first material used as absorber layer for solar cells was silicon, and later came Copper Indium Gallium Sulfur (GIGS), organic cells CdTe which are of the second generation [1-3]. The third and most recent generation is perovskite solar cells which has been show a better conversion and efficiency compared to others generations of solar cells. The general structure of perovskite is ABX_3 where A and B are cations and X is an anion. The cation A can be organic the Methylammonium ion (MA^+), the Formamidinium ion (FA+), or inorganic as the cesium (Cs). The cation B = lead (Pb^{2+}) or tin (Sn^{2+}) and the anion X = Iodide I^-, Bromide Br^-, or Chloride Cl^-. The Methylammonium Lead halide ($MAPbX_3$) investigated due to its higher power conversion efficiency, good optoelectronic properties, good absorption of light in UV-Visible and low cost [3-5].

This study will allow knowing the advantages and disadvantages of these three materials ($MAPbI_3$, $MAPbBr_3$, $MAPbCl_3$) deposited on zinc oxide (ZnO). Zinc oxide is a transparent material conductor with a large direct bandgap of 3.3 eV [6]. The ZnO film is an n-type that can be used as electron transport in solar cells and as catalytic and piezoelectric catalysis [7,8]. The manufacture of a solar cell can be achieved with Several techniques that can be used to produce the different layers, including the printing method, such as [7], inkjet [8], spray, dip-coating, spin-coating [9], etc. the spin-coating technique has been used in this investigation Due to its ease of use and low cost.

This work aims to study the effect of halogen X on the $MAPbX_3$ perovskite films where X can be iodine, bromide, or chloride on crystalline structure, surface morphology, and optical properties deposited by spin coating technique on the ZnO film. Further, the stability of the homojunction $MAPbX_3$/ZnO/FTO was investigated under dark conditions with 50% of humidity.

2- Experimental part

2.1- Films preparation

The different solutions were prepared using the appropriate precursors. The ZnO solution of concentration 0.5 M was prepared by dissolving zinc acetate [$Zn(CH_3COO)_2$, $2H_2O$] in ethanol. Three solutions of perovskite ($MAPbX_3$, X = I, Br, Cl) were also prepared. The lead halide (PbX_2), and methylammonium halide (MAX) were used to prepare the solution. The precursors

based-iodide was dissolved in N, N-dimethylformamide (DMF), and the precursors based-bromide and based-chloride were dissolved in dimethylsulfoxide (DMSO). The prepared zinc oxide solution was deposited by spin coating at a speed of 5000 rpm for 30 s on FTO glass substrates. The prepared ZnO films were annealed at 450º and then characterized. These films were reused for the deposition of perovskite solutions by the same method and under the same conditions. For perovskite deposits, we drop the Antisolvent diethyl ether a few seconds after the speed starts. The addition of Antisolvent diethyl ether will promote the solvent's vaporization, allowing the samples' good morphology and crystallinity.

2.2- Characterization of samples

The ZnO/$MAPbX_3$ heterojunction and the ZnO filmhave been characterized. The absorption and transmittance of samples were measured in the wavelength range of 300-900 nm with an Ocean Optic HR4000 spectrometer. The samples were characterized by X-ray diffraction using the device RIGAKU Ultima IV diffractometer. The device Scanning Field Emission Electron Microscope (FESEM) was used to examine the surface morphology under voltage conditions of 1.5 kV.

3- Results and discussions

3.1- X-ray diffraction analysis

The ZnO/$MAPbX_3$ heterojunction and the ZnO film were characterized by X-ray diffraction. The results are depicted in figure 1 below. Figure 1a shows two diffraction peaks of the ZnO thin film located at $2\theta = 33.57º$ and $2\theta = 37.61º$, corresponding respectively to the (002) and (101) planes of the hexagonal wurtzite structure (JCPDS Card Nº00-036-1451). From these XRD patterns, we can confirm that the ZnO thin films are polycrystalline. Moreover, figure 1a shows two diffraction peaks of the ZnO/$MAPbX_3$ heterojunction corresponding to the (100) and (200) for the crystallographic plane. These peaks are matching with what is reportedin the literature [10]. ZnO/$MAPbBr_3$ peaks are more intense and located at $2\theta = 14.96º$ and $2\theta = 30.13º$, respectively, for the (002) and (101) planes. ZnO/$MAPbI_3$ peaks are located at $2\theta = 12.66º$ and $2\theta = 28.3º$ respectively for the (002) and (101) planes and those of ZnO/$MAPbCl_3$ located at $2\theta = 11.05º$ and $2\theta = 32.23º$ respectively. The intense peaks with excellent resolutions of the bromine-based films show that these films are single-phase. The chlorine-based sample releases its first peak before those of the other films and its second peak after the second peak of the other two films. The peaks of the iodine-based films come out just before those of the

bromine-based films. Also, note the presence of ZnO peaks at the heterojunctions which shows that the ZnO/MAPbX$_3$ are indeed made of the two materials (zinc oxide and perovskite).

The curves of the maximum width at half maximum (FWHM) of the film products and for the crystallographic planes (100) and (200) are represented in figure 1b.

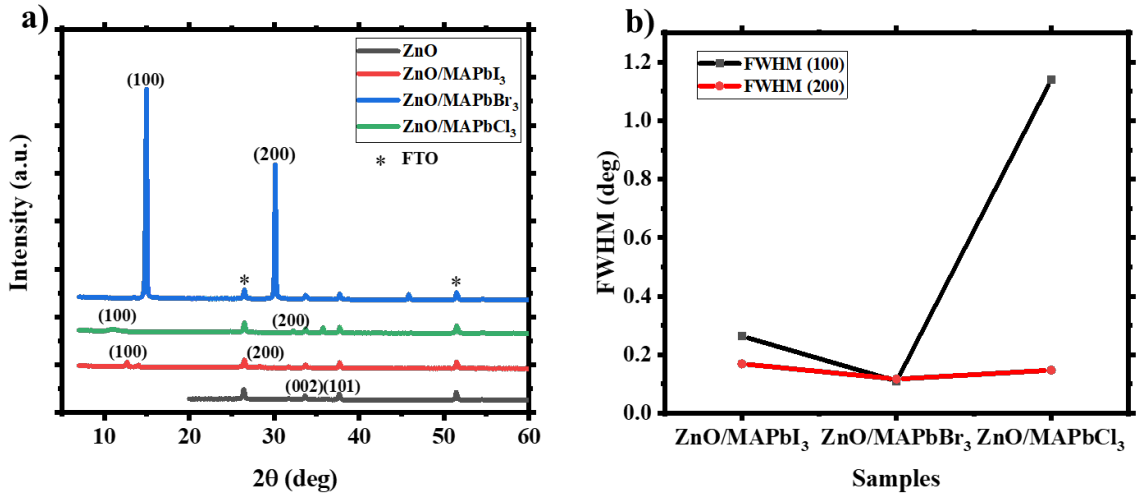

Figure 1: a) XRD patterns of ZnO/MAPbX$_3$ heterojunction, b) FWHM of ZnO /MAPbX$_3$ samples

Crystal lattice effective strain was determined to know the grains defects and strains in the thin films. Effective deformation of the network is determined using equation (1) below [11,12].

$$\beta\cos(\theta) = \frac{\lambda k}{D} + 4\varepsilon\sin(\theta) \quad (1)$$

Where β: FWHM; k =0.94; θ: Bragg angle; D: the grain size, and λ = 0.1540 nm: the wavelength of the X-ray.

Equation (2) was used to calculate the lattice dislocation density [13]:

$$\delta = \frac{1}{D^2} \quad (2)$$

The results of the different parameters calculated are summarized in table 1 below. Grains size D were given by XRD results.

Table 1: The XRD parameters of XRD spectra of ZnO and ZnO/$MAPbX_3$ films

Samples ID	Grains size D (nm)	Dislocation density δ (nm^{-2})	Lattice strain ε
ZnO	401	$6.22x10^{-6}$	0.173
ZnO/$MAPbI_3$	412	$5.89x10^{-6}$	0.382
ZnO/$MAPbI_2Br$	490		
ZnO/$MAPbI_2Cl$	551		

Table 1 shows that the grain sizes varyfrom 330 nm to 747 nm. The bromine-based sample has the largest grain size of 747 nm and the chlorine based-sample has the smallest grain size. The small values of the effective lattice from 0.159 to 0.382 of samples are explained by fewer deficiencies and distortions of the grains. Moreover, the samples ZnO and ZnO/$MAPbI_3$ which have the smallest lattice grain values show fewer grain defects and distortions than the other samples.

3.2- UV-Visible analysis

The absorption spectra of samples are illustrated in figure 2a in the range of 300 nm and 900 nm. The ZnO/$MAPbI_3$ sample has a higher absorption coefficient than the other samples. The absorption of the ZnO/$MAPbCl_3$ and ZnO/$MAPbBr_3$ heterojunction samples is around 0.25, the ZnO is less than 0.2. This difference in absorption coefficient would be explained by the light or dark shade of the different materials films and if it is film or heterojunction [14]. Indeed, the black color absorbs the most, and the sample iodine-based has a color that tends the most to black than the others will therefore absorb the most. The transmittance of the samples in figure 2b evolves well, contrary to the absorption. The single films have the highest transmittance of the order of 80 %. The band gaps, shown in figures 2c and 2d, were determined from the absorption data. Figure 2c shows the band gap of ZnO, which is 3.25 eV, close to that found in the literature (3.3 eV) [15]. The band gaps of the films depicted in figure 2d ranged from 1.95 eV for ZnO/MAPbI3 to 2.7 eV for ZnO/$MAPbCl_3$. The band gaps found are summarized in table 2 below. We used the Tauc equation to calculate the optical band gap Eg [16].

$$(\alpha h\nu)^2 = \beta\,(h\nu - Eg) \qquad (3)$$

In this equation, β is a constant independent of the energy hν and α is the absorption coefficient. We constructed the function $(\alpha h\nu)^2$ as a function of the energy hν to determine the bandgap by extrapolation.

The band gap of samples varies from 1.95 to 3.25 and is summarized in table 2 below.

Table 2:

Band gaps of ZnO and ZnO/MAPbX3 films samples calculated from UV-Visible

Samples ID	**Wavelength (nm)**	**Eg (eV)**
ZnO	381	3.25
$ZnO/MAPbI_3$	635	1.95
$ZnO/MAPbBr_3$	563	2.2
$ZnO/MAPbCl_3$	459	2.7

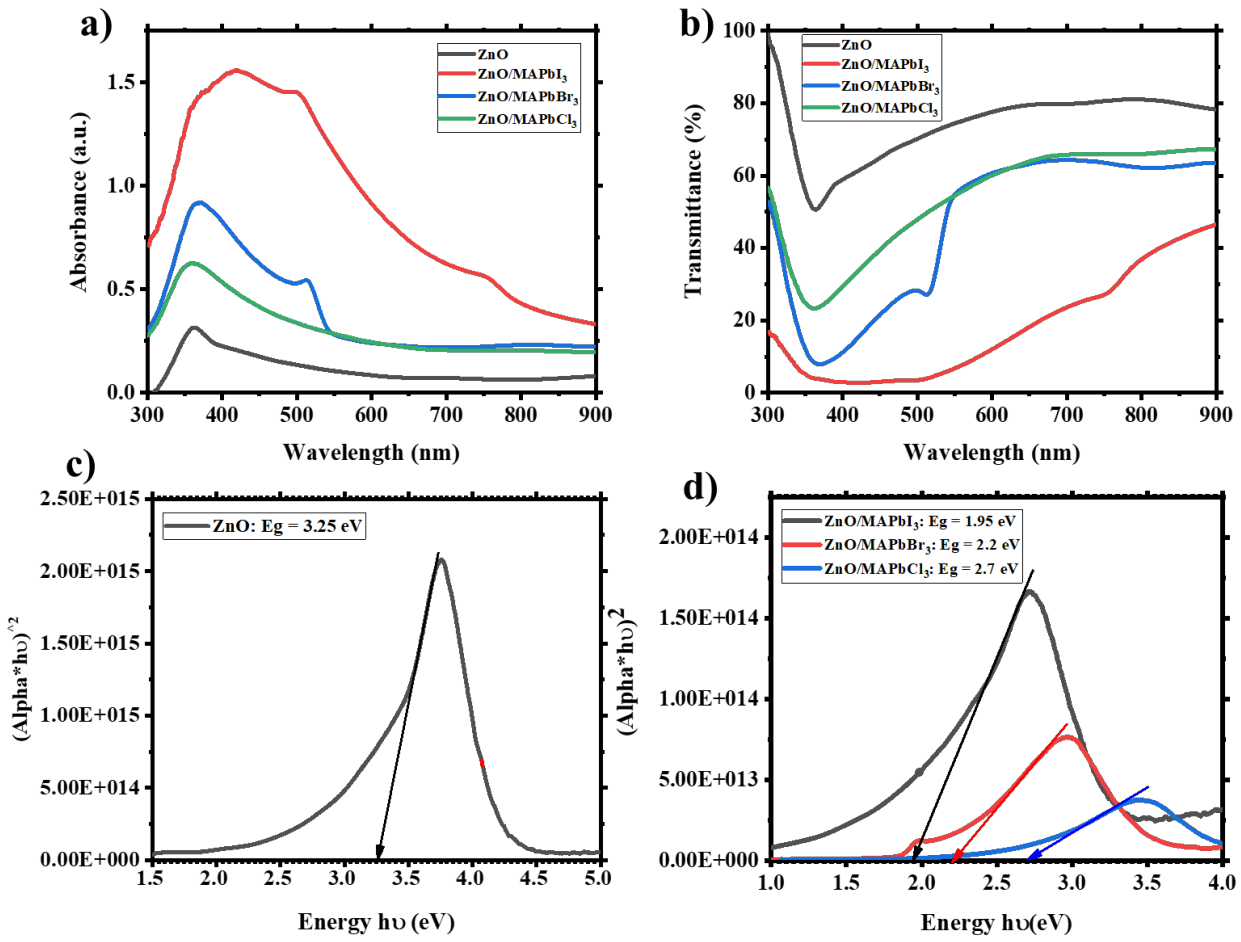

Figure 2: a) Absorption of ZnO and ZnO/MAPbX$_3$ films; b) transmittance of samples ZnO and ZnO/MAPbX$_3$ films; c-d) band gap of ZnO and ZnO/MAPbX$_3$ films

3.3- SEM analysis

SEM images of ZnO/MAPbX$_3$ where can X= I/ Br or Cl samples are shown in figure 3 . These images clearly show the crystalline character of the perovskite films and ZnO film produced, which is in good agreement with the X-ray diffraction results. Moreover, the images show that the grain size of the sample ZnO/MAPbBr$_3$ (figure 3c) is the largest of the grain sizes this had been shown previously by XRD data and This phenomenon is mainly due to the fact that the particles observed by SEM are composed of many grains. We can also see that a good distribution of the perovskite on the ZnO grains [17,18].

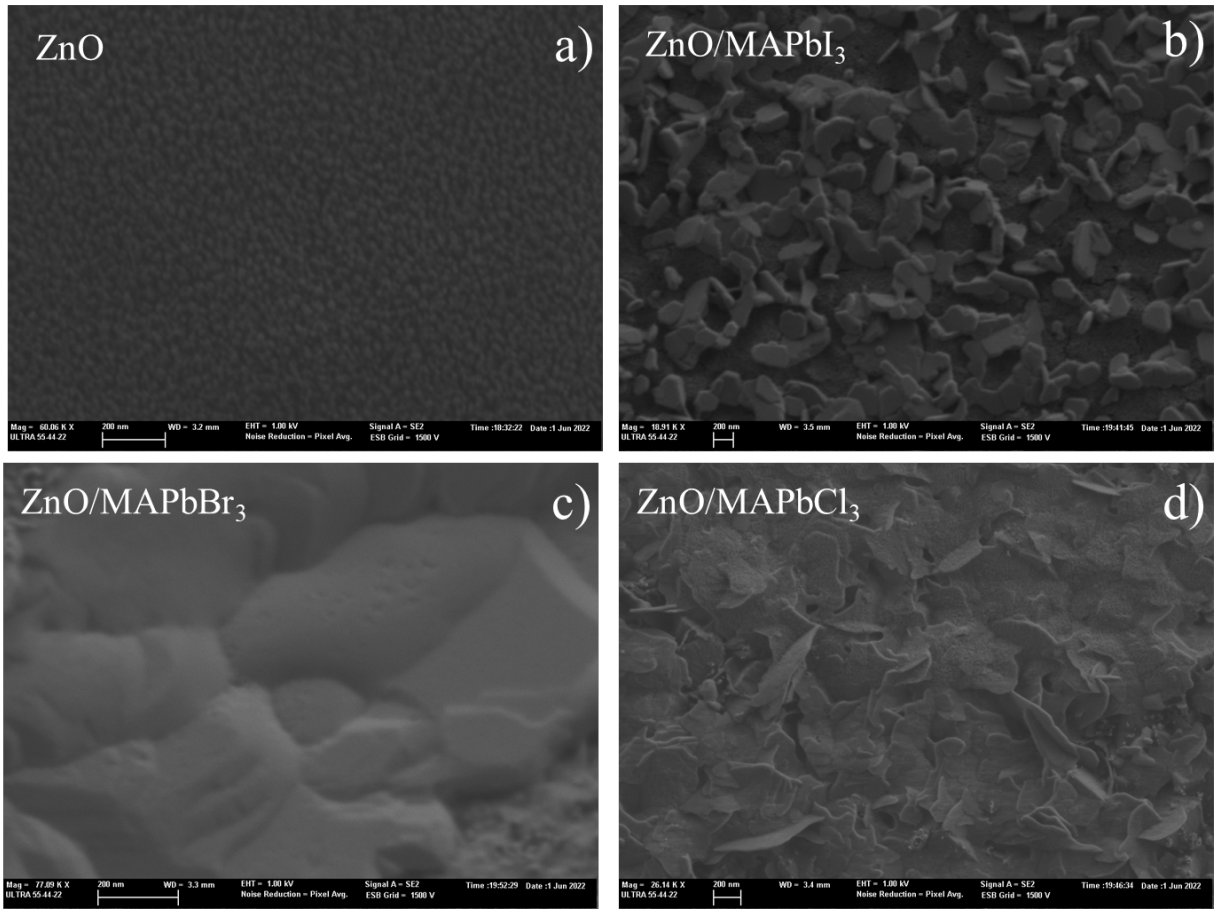

Figure 3: SEM images of a) ZnO; b) $ZnO/MAPbI_3$; c) $ZnO/MAPbBr_3$; d) $ZnO/MAPbCl_3$

4- Degradation study

The degradation mechanism of $ZnO/MAPbI_3$, ZnO/MAPbBr and $ZnO/MAPbCl_3$ samples is studied by XRD, SEM, and UV- Visible analysis . Figure 4 shows the photographs of the fresh and aged films. Oxygen and humidity are environmental factors that significantly affect the stability of perovskite-based solar cells [19].

$$MAPbX3 \quad \text{----------} \rightarrow MAX + PbX2 \qquad (4)$$

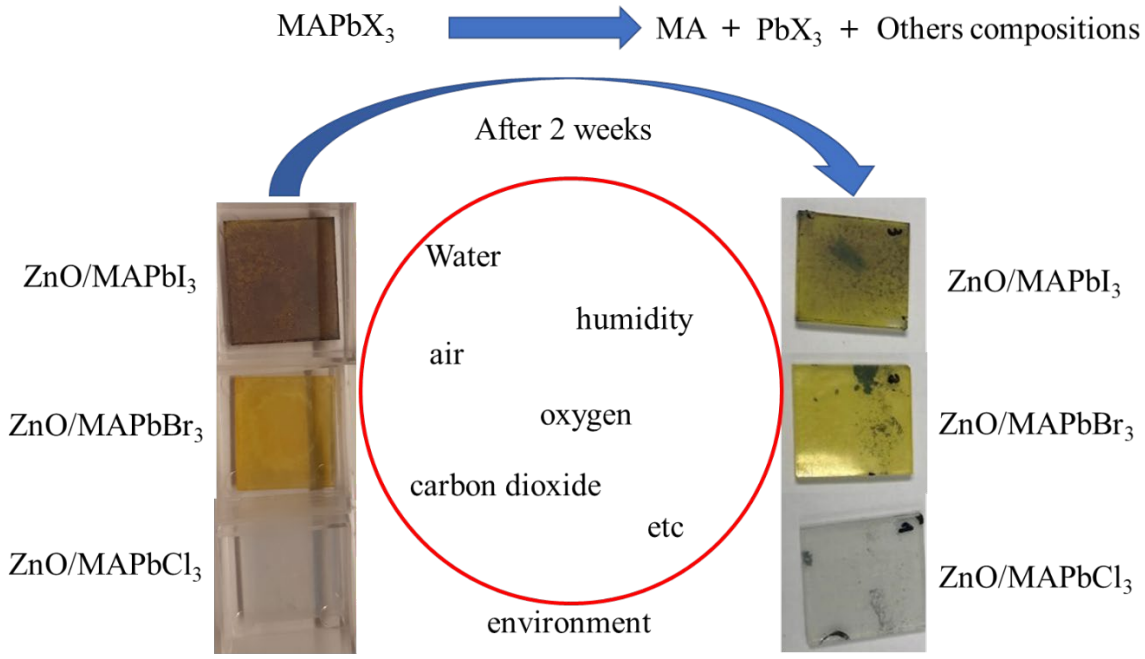

Figure 4: Process of degradation and photographs of fresh and aged $ZnO/MAPbX_3$ films after two weeks

Figure 5 below shows XRD patterns of fresh and aged methylammonium lead halide after two weeks under darks conditions. Results show that the intensities of the peaks of the $ZnO/MAPbI_3$ sample decreased significantly after two weeks compared to the other two samples: $ZnO/MAPbCl_3$ and $ZnO/MAPbBr_3$. Thus, X-ray analysis shows that the iodine-based sample is the least stable. The degradation is perceptible at the level of the perovskite layer which is very sensitive to humidity. The peaks of the ZnO layer do not experience a large change. zinc oxide is a much more stable material.

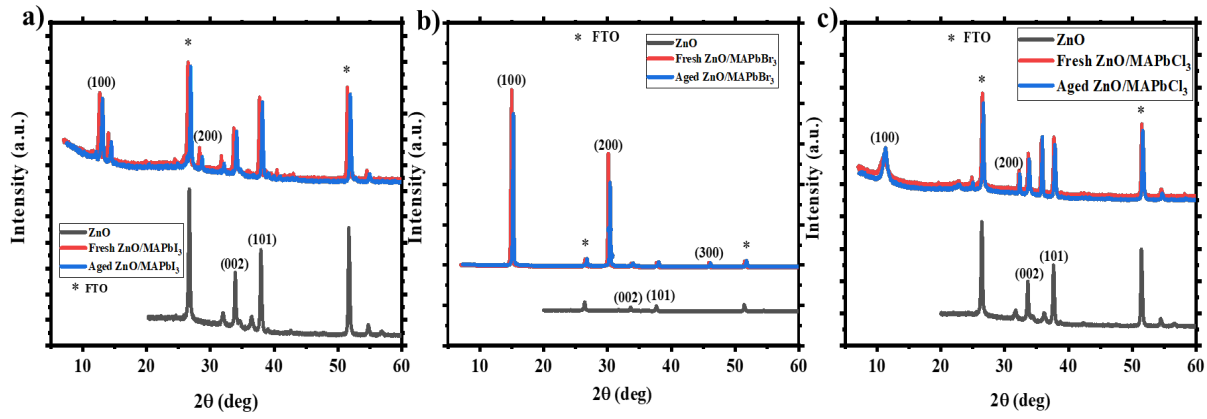

Figure 5: XRD patterns of fresh and aged methylammonium lead halide after two weeks: a) ZnO and ZnO/MAPbI3, b) ZnO and ZnO/MAPbBr3, c) ZnO and ZnO/MAPbCl3

The Absorption spectra of fresh and aged samples after two weeks are depicted in figure 6. Figure 6a ($ZnO/MAPbI_3$) shows a significant decrease in the absorption coefficient compared to the other two samples which match with the XRD results reported. Sample $ZnO/MAPbI_3$ deteriorated much more than the other two. These results are in good agreement with the photographs in figure 4 as well as with the X-ray diffraction analysis.

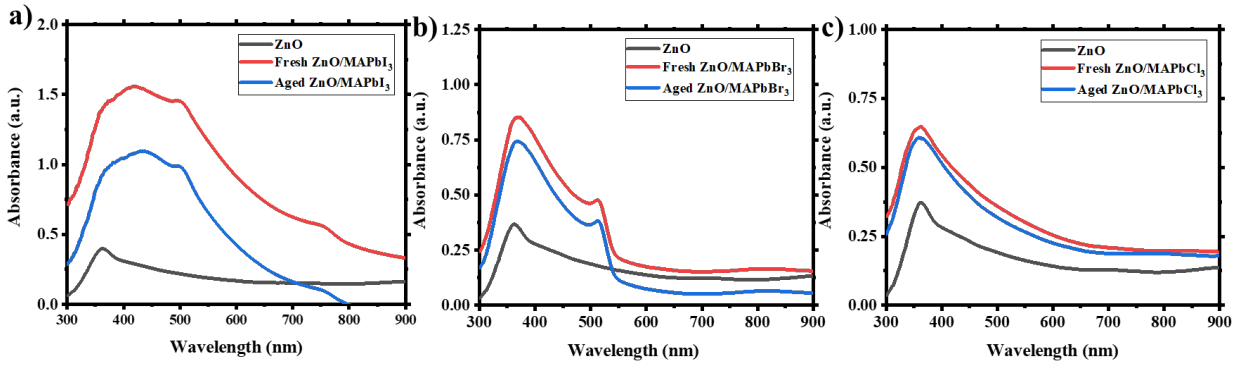

Figure 6: Absorption spectra of fresh and aged methylammonium lead halide after two weeks: a) ZnO and $ZnO/MAPbI_3$, b) ZnO and $ZnO/MAPbBr_3$, c) ZnO and $ZnO/MAPbCl_3$

The SEM images of the $ZnO/MAPbI_3$, ZnO and $ZnO/MAPbBr_3$ and $ZnO/MAPbCl_3$ samples were illustrated and are shown in figure 7. The different layers of perovskite experienced have been degraded during these two weeks. This degradation is due to the presence of water molecules. These water molecules lead to the decomposition of the $MAPbX_3$ perovskite into MAX and PbX_2. The degradation is clear in the SEM images (Figure 7) and even in the photos of the samples (Figure 4). The photographs of the samples show a color change due to their degradation. The SEM images confirm the degradation through the observed surface defects and holes. Among the different samples, the iodine-based sample is the most degraded, which agrees with the previous results by the absorption spectra and the XRD.

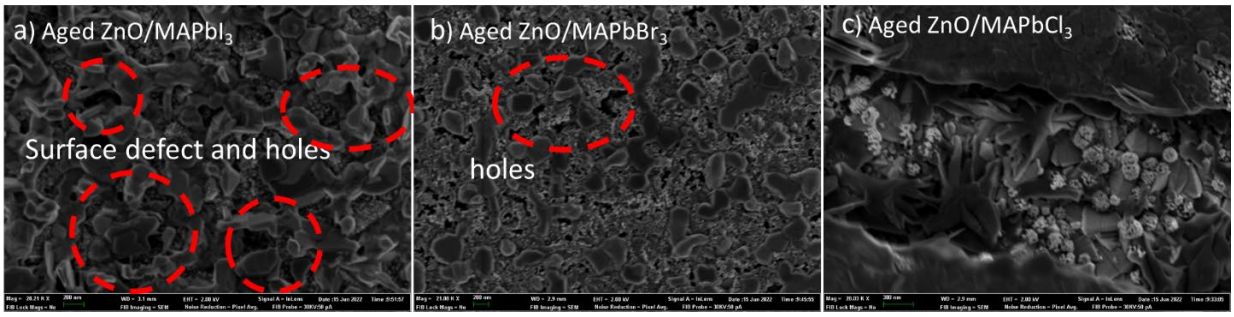

Figure 7: SEM images of degraded surfaces of different samples after two weeks: a) $ZnO/MAPbI_3$, b) $ZnO/MAPbBr_3$, c) $ZnO/MAPbCl_3$

Conclusion

This work investigated the influence of halogen X in methylammonium lead halide ($MAPbX_3$) examined by UV-visible, XRD, and SEM characterizations. Subsequently, the stability of the different samples was studied. This work reveals that the effect of halogen X is noticeable in $MAPbX_3$. The UV-visible characterization showed that the iodine-based sample absorbed the best and had a smaller band gap. XRD analysis shows two diffraction peaks of the $ZnO/MAPbX_3$ heterojunction corresponding to the (100) and (200) for the crystallographic plane. $ZnO/MAPbBr_3$ peaks are more intense than other sample peaks. This analysis also shows the crystalline character of the films produced, which is in good agreement with the SEM images. Both analyses (XRD and SEM) showed that the grain sizes of the sample $ZnO/MAPbBr_3$ are large. The degradation study showed that the iodine-based sample degrades faster.

Declaration of Competing Interest

The authors declare that they have no known competing financial interests or personal relationships that could have appeared to influence the work reported in this paper.

Acknowledgments

Author Klègayéré Emmanuel Koné thanks Erasmus + KA107 for the grant. Author Amal Bouich acknowledged the post-doctoral contract supported by the RRHH, the Postdoctoral contract Margarita Salas financed with the Union European Next Generation EU. This research has been funded by Grant PID2019-107137RB-C22 funded by MCIN/AEI/10.13039/501100011033 and by `` ERDF A way of making Europe´´.

References

[1] Oyedele, S., Boko, A. K. A., & Marí, B. (2017). Optimisation des paramètres photovoltaïques du CIGS al aide du simulateur AMPS-1D. *Afrique Science*, *13*(2), 274-283.

[2] Bouich, A., Marí-Guaita, J., Bouich, A., Pradas, I. G., & Marí, B. (2022). Towards manufacture stable lead perovskite APbI3 (A= Cs, MA, FA) based solar cells with low-cost techniques. *Engineering Proceedings*, *12*(1), 81.

[3] De Wolf, S., Holovsky, J., Moon, S. J., Loper, P., Niesen, B., Ledinsky, M., ... & Ballif, C. (2014). Organometallic halide perovskites: sharp optical absorption edge

and its relation to photovoltaic performance. *The journal of physical chemistry letters*, *5*(6), 1035-1039.

[4] Kumar, Y., Sanal, K. C., Perez, T. D., Mathews, N. R., & Mathew, X. (2019). Band offset studies in MAPbI3 perovskite solar cells using X-ray photoelectron spectroscopy. *Optical Materials*, *92*, 425-431.

[5] Olthof, S., & Meerholz, K. (2017). Substrate-dependent electronic structure and film formation of MAPbI3 perovskites. *Scientific reports*, *7*(1), 1-10.

[6] Gledhill, S., Grimm, A., Allsop, N., Koehler, T., Camus, C., Lux-Steiner, M., & Fischer, C. H. (2009). A spray pyrolysis route to the undoped ZnO layer of Cu (In, Ga)(S, Se) 2 solar cells. *Thin Solid Films*, *517*(7), 2309-2311.

[7] Wang, S., Tang, S., Yang, H., Wang, F., Yu, C., Gao, H., ... & Li, D. (2022). A novel heterojunction ZnO/CuO piezoelectric catalysts: fabrication, optical properties and piezoelectric catalytic activity for efficient degradation of methylene blue. Journal of Materials Science: Materials in Electronics, 33(9), 7172-7190.

8] Tang, S., Gao, H., Wang, S., Fang, L., Chen, X., Yang, H., ... & Yi, Z. (2022). Piezoelectric catalytic, photocatalytic and adsorption capability and selectivity removal of various dyes and mixed dye wastewater by ZnO nanoparticles. Main Group Chemistry, (Preprint), 1-19.

[9] Tang, M. C., Dang, H. X., Lee, S., Barrit, D., Munir, R., Wang, K., ... & Amassian, A. (2021). Wide and Tunable Bandgap MAPbBr3− xClx Hybrid Perovskites with Enhanced Phase Stability: In Situ Investigation and Photovoltaic Devices. *Solar RRL*, *5*(4), 2000718.

[10] Jang, D. M., Park, K., Kim, D. H., Park, J., Shojaei, F., Kang, H. S., ... & Song, J. K. (2015). Reversible halide exchange reaction of organometal trihalide perovskite colloidal nanocrystals for full-range band gap tuning. *Nano letters*, *15*(8), 5191-5199.

[11] Ullah, S., Bouich, A., Ullah, H., Mari, B., & Mollar, M. (2020). Enhanced optical and structural properties of V-doped binary SnS2 buffer layer. *Solar Energy*, *204*, 654-659.

[12] Ullah, S., Bouich, A., Ullah, H., Mari, B., & Mollar, M. (2020). Comparative study of binary cadmium sulfide (CdS) and tin disulfide (SnS2) thin buffer layers. *Solar Energy*, *208*, 637-642.

[13] Bouich, A., Hartiti, B., Ullah, S., Ullah, H., Ebn Touhami, M., Santos, D. M. F., & Mari, B. (2019). Optoelectronic characterization of CuInGa (S) 2 thin films grown by spray pyrolysis for photovoltaic application. *Applied Physics A*, *125*(8), 1-9.

[14] Fradi, K., Bouich, A., Slimi, B., & Chtourou, R. (2022). Towards improving the optoelectronics properties of MAPbI3 (1− x) B3x/ZnO heterojunction by bromine doping. *Optik*, *249*, 168283.

[15] Bouich, A., Marí-Guaita, J., Sahraoui, B., Palacios, P., & Marí, B. (2022). Tetrabutylammonium (TBA)-Doped Methylammonium Lead Iodide: High Quality and Stable Perovskite Thin Films. *Front. Energy Res*, *10*, 840817.

[16] Marí-Guaita, J., Bouich, A., Shafi, M. A., Bouich, A., & Marí, B. (2022). Investigation on the stability and efficiency of MAPbI3 and MASnI3 thin films for Solar Cells. *physica status solidi (a)*, *219*(5), 2100664.

[17] Wang, S. F., Zu, X. T., Sun, G. Z., Li, D. M., He, C. D., Xiang, X., ... & Li, S. (2016). Highly dispersed spinel (Mg, Ca, Ba)-ferrite nanoparticles: Tuning the particle size and magnetic properties through a modified polyacrylamide gel route. Ceramics International, 42(16), 19133-19140.

[18] Wang, S. F., Li, Q., Zu, X. T., Xiang, X., Liu, W., & Li, S. (2016). Phase controlled synthesis of (Mg, Ca, Ba)-ferrite magnetic nanoparticles with high uniformity. Journal of Magnetism and Magnetic Materials, 419, 464-475.

[19] Niu, G., Guo, X., & Wang, L. (2015). Review of recent progress in chemical stability of perovskite solar cells. *Journal of Materials Chemistry A*, *3*(17), 8970-8980.